

This article was downloaded by: [*Consorti de Biblioteques Universitaries de Catalunya*]

On: 14 December 2009

Access details: *Access Details: [subscription number 789296669]*

Publisher *Taylor & Francis*

Informa Ltd Registered in England and Wales Registered Number: 1072954 Registered office: Mortimer House, 37-41 Mortimer Street, London W1T 3JH, UK



International Journal of Control

Publication details, including instructions for authors and subscription information:

<http://www.informaworld.com/smpp/title~content=t713393989>

Simultaneous interconnection and damping assignment passivity-based control: the induction machine case study

Carles Batlle ^a; Arnau Dòria-Cerezo ^a; Gerardo Espinosa-Pérez ^b; Romeo Ortega ^c

^a MA4, DEE and IOC, UPC, Spain ^b DEPI-UNAM, México D.F., México ^c Laboratoire des Signaux et Systèmes, CNRS-SUPÉLEC, France

To cite this Article Batlle, Carles, Dòria-Cerezo, Arnau, Espinosa-Pérez, Gerardo and Ortega, Romeo(2009) 'Simultaneous interconnection and damping assignment passivity-based control: the induction machine case study', *International Journal of Control*, 82: 2, 241 – 255

To link to this Article: DOI: 10.1080/00207170802050817

URL: <http://dx.doi.org/10.1080/00207170802050817>

PLEASE SCROLL DOWN FOR ARTICLE

Full terms and conditions of use: <http://www.informaworld.com/terms-and-conditions-of-access.pdf>

This article may be used for research, teaching and private study purposes. Any substantial or systematic reproduction, re-distribution, re-selling, loan or sub-licensing, systematic supply or distribution in any form to anyone is expressly forbidden.

The publisher does not give any warranty express or implied or make any representation that the contents will be complete or accurate or up to date. The accuracy of any instructions, formulae and drug doses should be independently verified with primary sources. The publisher shall not be liable for any loss, actions, claims, proceedings, demand or costs or damages whatsoever or howsoever caused arising directly or indirectly in connection with or arising out of the use of this material.

Simultaneous interconnection and damping assignment passivity-based control: the induction machine case study

Carles Batlle^a, Arnau Dòria-Cerezo^a, Gerardo Espinosa-Pérez^{b*} and Romeo Ortega^c

^aMA4, DEE and IOC, UPC, EPSEVG, Av. V. Balaguer s/n, Vilanova i la Geltrú, 08800, Spain; ^bDEPFI-UNAM, Apartado Postal 70-256, 04510, México D.F., México; ^cLaboratoire des Signaux et Systèmes CNRS-SUPÉLEC, Gif-sur-Yvette, 91192, France

(Received 23 August 2007; final version received 12 March 2008)

We argue in this article that the standard two-stage procedure used in interconnection and damping assignment passivity-based control (IDA-PBC) – consisting of splitting the control action into the sum of energy-shaping and damping injection terms – is not without loss of generality, and effectively reduces the set of systems that can be stabilised with IDA-PBC. To overcome this problem we carry out, simultaneously, both stages and refer to this variation of the method as SIDA-PBC. To illustrate the application of SIDA-PBC we consider the practically important example given by the control problem of the induction machine. First, we show that torque and rotor flux regulation of the induction motor cannot be solved with two stage IDA-PBC. It is, however, solvable with SIDA-PBC. Second, we prove that with SIDA-PBC we can shape the total energy of the full (electrical and mechanical) dynamics of a doubly-fed induction generator used in power flow regulation tasks, while with two stage IDA-PBC only the electrical energy can be shaped. Simulation results of these examples are presented to illustrate the performance improvement obtained with SIDA-PBC.

Keywords: nonlinear control; passivity-based control; energy-shaping; induction machine

1. Introduction

Passivity-based control (PBC) is a generic name given to a family of controller design techniques that achieves system stabilisation via the route of passivation, that is, rendering the closed-loop system passive with a desired storage function (that usually qualifies as a Lyapunov function for the stability analysis.) If the passivity property turns out to be output strict, with an output signal with respect to which the system is detectable, then asymptotic stability is ensured. See the monographs (Ortega, Loria, Nicklasson and Sira-Ramírez 1998; van der Schaft 2002; Ortega and Garcia-Canseco 2004) for a recent survey.

As is well-known (van der Schaft 2002), a passive system can be rendered strictly passive simply by adding a negative feedback loop around the passive output – an action sometimes called L_gV control (Sepulchre, Janković and Kokotović 1997). For this reason, it has been found convenient in some applications, in particular for mechanical systems (Takegaki and Arimoto 1981; Ortega, Spong, Gomez and Blankenstein 2002a) to split the control action into the sum of two terms: an energy-shaping term which, as indicated by its name, is responsible of assigning the desired energy/storage function to the passive map; and a second L_gV term that injects damping for

asymptotic stability. The purpose of this article is to bring to the reader's attention the fact that splitting the control action in this way is not without loss of generality, and effectively reduces the set of problems that can be solved via PBC. This assertion, already recognised and proved in Prajna, van der Schaft and Meinsma (2002) for the linear systems case, is not surprising since it is clear that, to achieve strict passivity, the procedure described above is just one of many other possible ways. Our point is illustrated with the IDA-PBC design methodology proposed in Ortega, van der Schaft, Maschke and Escobar (2002b). To enlarge the set of systems that can be stabilised via IDA-PBC we suggest to carry out simultaneously the energy shaping and the damping injection stages and refer to this variation of the method as SIDA-PBC.

We illustrate the application of SIDA-PBC with the practically important example given by the control problem of induction machines operating both as a motor and as a generator. First, we show that the fundamental problem of induction motor torque and rotor flux regulation cannot be solved with two stage IDA-PBC. It is, however, solvable with SIDA-PBC. Second, we prove that with SIDA-PBC we can shape the total energy of the full (electrical and mechanical) dynamics of a doubly-fed induction generator used in

*Corresponding author. Email: gerardoe@servidor.unam.mx

power flow regulation tasks while, as reported in Batlle, Dòria-Cerezo and Ortega (2005), with two stage IDA–PBC only the electrical energy could be shaped. Simulation results of these examples are presented to illustrate the performance improvement obtained with SIDA–PBC.

2. Simultaneous energy-shaping and damping injection control

We consider the problem of stabilisation of an equilibrium point for non-linear systems of the form

$$\dot{x} = f(x, t) + g(x)u, \quad (1)$$

where $x \in \mathbb{R}^n$ is the state vector, $u \in \mathbb{R}^m$, $m < n$, is the control action and $g(x)$ is assumed full rank. In two-stage IDA–PBC this objective is achieved as follows; see Ortega et al. (2002a) and Ortega et al. (2002b) for further details. First, decompose the control signal in two terms

$$u = u_{es} + u_{di}, \quad (2)$$

where u_{es} is responsible of the energy-shaping stage and u_{di} injects the damping. Second, solve the key matching equation¹

$$g^\perp(x)f(x, t) = g^\perp(x)J_d(x, t)\nabla H_d \quad (3)$$

for some functions

$$J_d: \mathbb{R}^n \times \mathbb{R} \rightarrow \mathbb{R}^{n \times n}, \quad H_d: \mathbb{R}^n \rightarrow \mathbb{R},$$

satisfying the skew-symmetry condition for the interconnection matrix

$$J_d(x, t) + J_d^\top(x, t) = 0, \quad (4)$$

and the equilibrium assignment condition for the desired total stored energy

$$x_\star = \arg \min H_d(x) \quad (5)$$

with $x_\star \in \mathbb{R}^n$ the equilibrium to be stabilised² and $g^\perp(x) \in \mathbb{R}^{(n-m) \times n}$ a full-rank left-annihilator of $g(x)$, that is $g^\perp(x)g(x) = 0$ and $\text{rank } g^\perp(x) = n - m$.

As shown in Ortega et al. (2002b) system (1) in closed-loop with the control (2), with

$$u_{es} = [g^\top(x)g(x)]^{-1}g^\top(x)\{J_d(x, t)\nabla H_d - f(x, t)\}, \quad (6)$$

yields a port-controlled Hamiltonian (PCH) system of the form

$$\left. \begin{aligned} \dot{x} &= J_d(x, t)\nabla H_d + g(x)u_{di} \\ y &= g^\top(x)\nabla H_d. \end{aligned} \right\} \quad (7)$$

The system (7) without a damping injection term is conservative, i.e., $\dot{H}_d = 0$, with x_\star a stable equilibrium

(with Lyapunov function $H_d(x)$). To add dissipation we fed back the passive output y , for instance, with

$$u_{di} = -K_{di}y, \quad K_{di} = K_{di}^\top > 0,$$

to finally obtain the PCH system with dissipation

$$\left. \begin{aligned} \dot{x} &= [J_d(x, t) - R_d(x)]\nabla H_d + g(x)v \\ y &= g^\top(x)\nabla H_d. \end{aligned} \right\} \quad (8)$$

where the damping matrix $R_d(x) = R_d^\top(x) \geq 0$ is defined by

$$R_d(x) = g(x)K_{di}g^\top(x),$$

and we have added a signal v to (2) to define the port variables. Since the new closed-loop system (with $v = 0$) satisfies $\dot{H}_d = -y^\top K_{di}y$, it is easy to prove (e.g., Lemma 3.2.8 of van der Schaft (2002)) that the equilibrium x_\star will now be asymptotically stable if it is detectable from y , i.e., if the implication ($y(t) \equiv 0 \Rightarrow \lim_{t \rightarrow \infty} x(t) = x_\star$) is true.

Obviously, the key for the success of IDA–PBC is the solution of the matching Equation (3). With the motivation of enlarging the class of systems for which this equation is solvable, in this article we propose to avoid the decomposition of the control into energy-shaping and damping injection terms. Instead, we suggest carrying out, simultaneously, both stages and replacing (3), with the SIDA–PBC matching equations

$$g^\perp(x)f(x, t) = g^\perp(x)F_d(x, t)\nabla H_d, \quad (9)$$

to replace the constraint (4) by the strictly weaker condition

$$F_d(x, t) + F_d^\top(x, t) \leq 0, \quad (10)$$

and defining the control as

$$u = [g^\top(x)g(x)]^{-1}g^\top(x)\{F_d(x, t)\nabla H_d - f(x, t)\}.$$

Since the set of skew-symmetric matrices is strictly contained in the set of matrices with negative semi-definite symmetric part, it is clear that the set of functions $\{f(x, t), g(x)\}$ for which (3) – subject to the constraint (4) – is solvable is strictly smaller than the set for which (9), subject to (10), is solvable.

Remark 1: There exist several techniques to solve the matching Equation (3) (resp. (9)), with two extremes being the purely algebraic approach of Fujimoto and Sugie (2001) and the PDE approach of Ortega et al. (2002b). In the former $H_d(x)$ is *a priori* fixed, which makes (3) (resp. (9)) an algebraic equation that is solved for $J_d(x, t)$ (resp. $F_d(x, t)$) – subject to the constraint (4) (resp. (10)). On the other hand, in the latter $J_d(x, t)$ (resp. $F_d(x, t)$) is fixed, making (3) (resp. (9)) a PDE that is solved for $H_d(x)$. We refer the interested reader to Ortega and Garcia-Canseco (2004) for a detailed discussion on these methods of solution

of the matching equations (as well as others). In this article we will adopt the algebraic approach.

Remark 2: Similarly to IDA–PBC, application of SIDA–PBC also yields a closed-loop PCH system of the form (8) with

$$J_d(x, t) = \frac{1}{2}[F_d(x, t) - F_d^\top(x, t)],$$

$$R_d(x, t) = \frac{1}{2}[F_d(x, t) + F_d^\top(x, t)].$$

Remark 3: To make IDA–PBC applicable to non-autonomous systems, which will be required in the induction motor application, we have presented, above, a slight variation of the method. Notice that the matrices J_d and R_d may depend explicitly on time. Clearly, their skew-symmetry and non-negativity properties must now hold uniformly in time as well.

3. Induction motor control via SIDA–PBC

In this section we will show that the problem of output feedback torque control of induction motors with quadratic in the increments desired energy function is not solvable via two-stage IDA–PBC. That is, it is not possible to solve (3) subject to (4). On the other hand, we will find a solution of (9) subject to (10), hence the problem is solvable with SIDA–PBC. An interesting feature of our SIDA–PBC is that, in contrast with the large majority of controllers proposed for the induction motor where signal convergence is inferred from the stability analysis of some kind of error dynamics (Marino, Peresada and Valigi 1993; Dawson and Burg 1998; Ortega et al. 1998), we establish here (Lyapunov) stability of a given equilibrium that generates the desired torque and rotor flux amplitude.

3.1 Motor model, control objective and equilibria

The standard three-phase induction motor represented with a two-phase model defined in an arbitrary reference frame, which rotates at an arbitrary speed $\omega_s \in \mathbb{R}$, is given by (Krause, Wasynczuk and Sudhoff 1995)

$$\dot{x}_{12} = -[\gamma I_2 + (n_p \omega + u_3) \mathcal{J}]x_{12} + \alpha_1(I_2 - T_r n_p \omega \mathcal{J})x_{34} + \alpha_2 u_{12} \quad (11)$$

$$\dot{x}_{34} = -\left(\frac{1}{T_r} I_2 + \mathcal{J} u_3\right)x_{34} + \frac{L_{sr}}{T_r} x_{12} \quad (12)$$

$$\dot{\omega} = \alpha_3 x_{12}^\top \mathcal{J} x_{34} - \frac{\tau_L}{J_m} \quad (13)$$

in which

$$I_2 = \begin{bmatrix} 1 & 0 \\ 0 & 1 \end{bmatrix}, \quad \mathcal{J} = \begin{bmatrix} 0 & -1 \\ 1 & 0 \end{bmatrix} = -\mathcal{J}^\top,$$

$x_{12} \in \mathbb{R}^2$ are the stator currents, $x_{34} \in \mathbb{R}^2$ the rotor fluxes, $\omega \in \mathbb{R}$ the rotor speed, $u_{12} \in \mathbb{R}^2$ are the stator voltages, $\tau_L \in \mathbb{R}$ is the load torque and $u_3 := \omega_s - n_p \omega$. The parameters, all positive, are defined as

$$\gamma := \frac{R_s}{L_s \sigma} + \frac{L_{sr}^2}{\sigma L_s L_r T_r}, \quad \sigma := 1 - \frac{L_{sr}^2}{L_s L_r}, \quad \alpha_1 := \frac{L_{sr}}{\sigma L_s L_r T_r},$$

$$\alpha_2 := \frac{1}{\sigma L_s}, \quad \alpha_3 := \frac{n_p L_{sr}}{J_m L_r}, \quad T_r := \frac{L_r}{R_r}$$

with L_s , L_r the windings inductances, R_s , R_r the windings resistances and L_{sr} the mutual inductance, n_p the number of pole pairs and J_m the rotor moment of inertia.

As first pointed out in the control literature in Ortega and Espinosa (1993), the signal u_3 (known in the drives literature as slip frequency) effectively acts as an additional control input. Below, we will select u_3 to transform the periodic orbits of the system into constant equilibria.

We are interested, in this article, in the problem of regulation of the motor torque and the rotor flux amplitude

$$y = \begin{bmatrix} y_1 \\ y_2 \end{bmatrix} = \begin{bmatrix} J_m \alpha_3 x_{12}^\top \mathcal{J} x_{34} \\ |x_{34}| \end{bmatrix}, \quad (14)$$

to some constant desired values $y_\star = \text{col}(y_{1\star}, y_{2\star})$, where $|\cdot|$ is the Euclidean norm. The following important practical restriction of the induction motor control problem has to be imposed:

(OF) The only signals available for measurement are x_{12} and ω .

To solve this problem using (S)IDA–PBC it is necessary to express the control objective in terms of a desired equilibrium. As is well-known (Marino et al. 1993), the zero dynamics of the induction motor is periodic, a fact that is clearly shown computing the angular speed of the rotor flux

$$\dot{\rho} = \frac{R_r y_1}{n_p y_2^2} - u_3,$$

where $\rho := \arctan(x_4/x_3)$ is the rotor flux angle. From this relation it is clear that, if u_3 is fixed to a constant, say \bar{u}_3 , and $y = y_\star$, x_{34} is a vector of constant amplitude rotating at speed $\rho(t) = ((R_r/n_p)(y_{1\star}/y_{2\star}^2) - \bar{u}_3)t + \rho(0)$. Therefore, the only choice of u_3 for which a (constant) equilibrium – compatible with the desired outputs y_\star – exists is

$$u_3 = u_{3\star} := \frac{R_r y_{1\star}}{n_p y_{2\star}^2}. \quad (15)$$

From this observation and (12) we have the following simple lemma whose proof is obtained via direct substitution.

Lemma 1: Consider the induction motor model (11)–(13) with output functions (14) and $u_3 = u_{3\star}$. Then, the set of assignable equilibrium points, denoted $\text{col}(\bar{x}_{12}, \bar{x}_{34}, \bar{\omega}) \in \mathbb{R}^5$, which are compatible with the desired outputs y_\star is defined by

$$\left. \begin{aligned} \bar{x}_{12} &= \frac{1}{L_{sr}} \begin{bmatrix} 1 & -\frac{L_r y_{1\star}}{n_p y_{2\star}^2} \\ \frac{L_r y_{1\star}}{n_p y_{2\star}^2} & 1 \end{bmatrix} \bar{x}_{34} \\ |\bar{x}_{34}| &= y_{2\star} \end{aligned} \right\} \quad (16)$$

with $\bar{\omega}$ arbitrary.

Among the set of assignable equilibria defined above we select, for the electrical coordinates, the one that

$$f(x, t) = \begin{bmatrix} -[\gamma I_2 + (n_p \omega(t) + u_{3\star})\mathcal{J}]x_{12} + \alpha_1 (I_2 - T_r n_p \omega(t)\mathcal{J})x_{34} \\ -\left(\frac{1}{T_r} I_2 + \mathcal{J}u_{3\star}\right)x_{34} + \frac{L_{sr}}{T_r} x_{12} \end{bmatrix}, \quad g = \alpha_2 \begin{bmatrix} I_2 \\ 0_{2 \times 2} \end{bmatrix}.$$

ensures field orientation (Krause et al. 1995) and, defining $x := \text{col}(x_{12}, x_{34})$, denote it

$$x_\star := \text{col}\left(\frac{y_{2\star}}{L_{sr}}, \frac{L_r y_{1\star}}{n_p L_{sr} y_{2\star}}, y_{2\star}, 0\right). \quad (17)$$

Remark 4: From (13) and (14) we see that to operate the system in equilibrium, $y_{1\star} = \tau_L$ (hence, to define the desired equilibrium) the load torque needs to be known. In practical applications, an outer loop PI control around the velocity error is usually added. The output of the integrator, on one hand, provides an estimate of τ_L while, on the other hand, ensuring that speed also converges to the desired value as shown via simulations in Section 3.5.

3.2 Algebraic (S)IDA–PBC problem formulation

As indicated in Remark 1, in this article we will adopt the algebraic approach to solve the matching equations. Fixing $f(x, t)$, $g^\perp(x)$ and $H_d(x)$, the two algebraic Equations, (3) and (9), are the same and the difference between IDA–PBC and SIDA–PBC depends only on the constraints imposed on the matrices $J_d(x, t)$ and $F_d(x, t)$. To simplify the problem formulation, we will use the generic symbol $F(x, t)$ to denote either $J_d(x, t)$ or $F_d(x, t)$. The distinction will be made imposing either $F(x, t) + F^\top(x, t) = 0$ or $F(x, t) + F^\top(x, t) \leq 0$, respectively.

Since we are interested, here, in torque control, and this is only defined by the stator currents and the rotor fluxes, its regulation can be achieved applying IDA–PBC to the electrical subsystem only. Boundedness of ω will be established in a subsequent analysis.

Although with IDA–PBC it is possible, in principle, to assign an arbitrary energy function to the electrical subsystem, we will consider for simplicity a quadratic in errors form

$$H_d(x) = \frac{1}{2}(x - x_\star)^\top P(x - x_\star), \quad (18)$$

with $P = P^\top > 0$ a matrix to be determined. As indicated in Remark 1, fixing $H_d(x)$ transforms the matching Equation (3) into a set of algebraic equations – see also Rodriguez and Ortega (2003) for application of this, so-called ‘Algebraic IDA–PBC’, to general electro-mechanical systems.

The electrical subsystem (11), (12) with $u_3 = u_{3\star}$ can be written in the form (1) with $u = u_{12}$, and

Notice that we are treating the dependence of the dynamics on angular speed ω as a time-dependence.

Since $g^\perp = [0_{2 \times 2} \quad I_2]$, the matching Equations (3) and (9) concern only the third and fourth rows of $f(x, t)$ and they take the form

$$-\left(\frac{1}{T_r} I_2 + \mathcal{J}u_{3\star}\right)x_{34} + \frac{L_{sr}}{T_r} x_{12} = [F_3(x, t) \quad F_4(x, t)]P(x - x_\star), \quad (19)$$

where, to simplify the notation, we partition $F(x, t)$ into 2×2 sub-matrices as

$$F(x, t) = \begin{bmatrix} F_1(x, t) & F_2(x, t) \\ F_3(x, t) & F_4(x, t) \end{bmatrix}. \quad (20)$$

The output feedback condition (OF) imposes an additional constraint that involves now the first and second rows of $f(x, t)$. Indeed, from (6) we see that the control can be written as

$$\alpha_2 u_{12} = [\gamma I_2 + (n_p \omega(t) + u_3)\mathcal{J}]x_{12} - \alpha_1 (I_2 - T_r n_p \omega(t)\mathcal{J})x_{34} + [F_1(x, t) \quad F_2(x, t)]P(x - x_\star).$$

Factoring the components that depend on the unmeasurable quantity x_{34} we can express u_{12} as

$$u_{12} = \hat{u}_{12}(x_{12}, \omega) + \frac{1}{\alpha_2} S(x, t)x_{34},$$

where we have defined

$$S(x, t) := \alpha_1 [T_r n_p \omega(t) \mathcal{J} - I_2] + F_1(x, t) P_2 + F_2(x, t) P_3,$$

partitioned P as

$$P := \begin{bmatrix} P_1 & P_2 \\ P_2^\top & P_3 \end{bmatrix}, \quad P_i \in \mathbb{R}^{2 \times 2}, \quad i = 1, 2, 3,$$

and defined a function, $\hat{u}_{12}(x_{12}, \omega)$, whose expression is given in (29). It is clear that, to verify the output feedback condition (OF), $S(x, t)$ has to be set to zero, that is

$$\alpha_1 [T_r n_p \omega(t) \mathcal{J} - I_2] + F_1(x, t) P_2 + F_2(x, t) P_3 = 0. \tag{21}$$

(S)IDA–PBC Problems. Find matrices $F(x, t)$ and $P = P^\top > 0$ satisfying (19)–(21) with the additional constraint that

- (Energy-shaping)

$$F(x, t) + F^\top(x, t) = 0, \tag{22}$$

or the strictly weaker

- (Simultaneous energy-shaping and damping injection)

$$F(x, t) + F^\top(x, t) \leq 0. \tag{23}$$

3.3 Solvability of the (S)IDA–PBC problems

Proposition 1: *The energy-shaping problem is not solvable. However, the simultaneous energy-shaping and damping injection one is solvable.*

Proof: First, we write the matching Equation (19) in terms of the errors

$$\begin{aligned} & \frac{L_{sr}}{T_r} (x_{12} - x_{12\star}) - \left(\frac{1}{T_r} I_2 + u_{3\star} \mathcal{J} \right) (x_{34} - x_{34\star}) \\ &= [F_3(x, t) \quad F_4(x, t)] P (x - x_\star), \end{aligned}$$

which will be satisfied if and only if

$$[F_3(x, t) \quad F_4(x, t)] P = \begin{bmatrix} \frac{L_{sr}}{T_r} I_2 & - \left(\frac{1}{T_r} I_2 + u_{3\star} \mathcal{J} \right) \end{bmatrix}. \tag{24}$$

Since P is full rank and the right hand side of the equation is constant, we conclude that F_3 and F_4 should also be constant. (To underscore the ‘nature’ of the F_i matrices we will explicitly write their arguments in the sequel.)

Let us first consider the energy-shaping problem. From (20) and (22) we have that $F_2 = -F_3^\top$. Replacing the latter in (21) it is obtained that

$$F_1(x, t) P_2 - F_3^\top P_3 = \alpha_1 [I_2 - T_r n_p \omega(t) \mathcal{J}]. \tag{25}$$

On the other hand, from the first two columns of (24) it follows that

$$F_3 = \left(\frac{L_{sr}}{T_r} I_2 - F_4 P_2^\top \right) P_1^{-1}. \tag{26}$$

Substitution of (26) into (25) leads to

$$F_1(x, t) P_2 - P_1^{-1} \left(\frac{L_{sr}}{T_r} I_2 - F_4 P_2^\top \right) P_3 = \alpha_1 I_2 - \alpha_1 T_r n_p \omega(t) \mathcal{J}. \tag{27}$$

Again, invoking (22) we have that $F_1(x, t)$ must be skew-symmetric. Furthermore, since it is only a function of t we can, without loss of generality, express it in the form

$$F_1(t) = \beta_1(t) \mathcal{J} + \beta_2 \mathcal{J},$$

where $\beta_2 \in \mathbb{R}$. Looking at the t -dependent terms we get

$$\beta_1(t) \mathcal{J} P_2 + \alpha_1 T_r n_p \omega(t) \mathcal{J} = 0,$$

which can be achieved only if $P_2 = \lambda I_2$, with $\lambda \in \mathbb{R}$, $\lambda \neq 0$, and $\beta_1(t) = -\lambda^{-1} \alpha_1 T_r n_p \omega(t)$.

The constant part of (27), considering that $P_2 = \lambda I_2$, reduces to

$$\lambda \beta_2 \mathcal{J} - P_1^{-1} \left(\frac{L_{sr}}{T_r} I_2 - \lambda F_4^\top \right) P_3 = \alpha_1 I_2$$

which – using the fact that P_3 is full rank – can be expressed as $F_4^\top = G P_3^{-1}$, where we have defined the constant matrix

$$G := \frac{1}{\lambda} \left[\frac{L_{sr}}{T_r} P_3 + P_1 (\alpha_1 I_2 - \lambda \beta_2 \mathcal{J}) \right].$$

Finally, since F_4 must also be skew-symmetric, we have that

$$G = P_3^{-1} (-G^\top) P_3.$$

Consequently, G must be similar to $-G^\top$, and both necessarily have the same eigenvalues. A necessary condition for the latter is that $\text{trace}(G) = 0$, that is not satisfied because

$$\text{trace}(G) = \frac{1}{\lambda} \left[\frac{L_{sr}}{T_r} \underbrace{\text{trace}(P_3)}_{>0} + \alpha_1 \underbrace{\text{trace}(P_1)}_{>0} \right],$$

which is different from zero. This completes the proof of the first claim.

We will now prove that if we consider the larger class of matrices (23) the problem is indeed solvable, and actually give a very simple explicit expression

for $F(x)$ and P . For, we set $P_2=0$, thus it is easy to see that

$$\begin{aligned} F_2(t) &= \alpha_1 [I_2 - T_r n_p \omega(t) \mathcal{J}] P_3^{-1} \\ F_3 &= \frac{L_{sr}}{T_r} P_1^{-1} \\ F_4 &= -\left(\frac{1}{T_r} I_2 + u_{3\star} \mathcal{J}\right) P_3^{-1} \end{aligned}$$

with $F_1(x, t)$, P_1 , P_3 free, provide a solution to (24) and (21). It only remains to establish (23). For this, we fix $P_1 = (L_{sr}/T_r)I_2$, $P_3 = \alpha_1 I_2$ and $F_1(t) = -\mathcal{K}(\omega(t))$, with $\mathcal{K}(\omega(t)) = \mathcal{K}^\top(\omega(t)) > 0$, then

$$F(t) = \begin{bmatrix} -\mathcal{K}(\omega(t)) & I_2 - T_r n_p \omega(t) \mathcal{J} \\ I_2 & -\alpha_1^{-1} \left(\frac{1}{T_r} I_2 + u_{3\star} \mathcal{J} \right) \end{bmatrix}.$$

A simple Schur complement analysis shows that $F(t) + F^\top(t) < 0$ if and only if

$$\mathcal{K}(\omega(t)) > \frac{L_{sr}}{L_s L_r - L_{sr}^2} \left[1 + \frac{1}{4} (T_r n_p \omega(t))^2 \right] I_2. \quad (28)$$

3.4 Proposed controller and stability analysis

Once the solvability of the SIDA–PBC problem has been established, the final part of the design is the explicit definition of the resulting controller and the assessment of its stability properties. This is summarised in the proposition below whose proof follows immediately from analysis of the closed-loop electrical sub-system $\dot{x} = F(t)\nabla H_d$ and the mechanical dynamics (13), where H_d is given by (18) and $F(t) + F^\top(t) < 0$.

Proposition 2: *Consider the induction motor model (11)–(13) with outputs to be regulated given by (14). Assume that*

- A.1 *the measurable states are the stator currents x_{12} and the rotor speed ω ,*
- A.2 *all the motor parameters are known,*
- A.3 *the load torque is constant and known.*

Fix the desired equilibrium to be stabilised as (17), with $y_\star = \text{col}(\tau_L, y_{2\star})$, $y_{2\star} > 0$, and set $u_3 = (R_r/n_p)(y_{1\star}/y_{2\star}^2)$ and $u_{12} = \hat{u}_{12}(x_{12}, \omega)$ with

$$\begin{aligned} \hat{u}_{12}(x_{12}, \omega) &= \frac{1}{\alpha_2} [\gamma I_2 + (n_p \omega + u_{3\star}) \mathcal{J}] x_{12} \\ &\quad - \frac{\alpha_1}{\alpha_2} (I_2 - T_r n_p \omega \mathcal{J}) x_{34\star} \\ &\quad - \frac{L_{sr}}{\alpha_2 T_r} \mathcal{K}(\omega) (x_{12} - x_{12\star}) \end{aligned} \quad (29)$$

and $\mathcal{K}(\omega)$ satisfying (28). Then, x_\star is a globally exponentially stable equilibrium of the x -subsystem with Lyapunov function

$$H_d(x) = \frac{L_{sr}}{2T_r} |x_{12} - x_{12\star}|^2 + \frac{\alpha_1}{2} |x_{34} - x_{34\star}|^2,$$

that satisfies $\dot{H}_d \leq -\kappa H_d$, for some $\kappa > 0$. Consequently, for all initial conditions,

$$\lim_{t \rightarrow \infty} x(t) = x_\star, \quad \lim_{t \rightarrow \infty} y(t) = y_\star,$$

exponentially fast. Furthermore, ω remains bounded and converges to some constant value, that is, $\lim_{t \rightarrow \infty} \omega(t) = \omega_\infty$.

Remark 5: The resulting SIDA–PBC is a simple output feedback scheme that ensures global exponential stability of the desired equilibrium, hence exponential convergence of the generated torque and the rotor flux norm to their desired (constant) values. To the best of our knowledge, this is the first output feedback scheme that ensures such strong stability properties for this system. Although, for the establishment of the theoretical result it is assumed that τ_L is known, as indicated in Remark 4 and further validated in the simulations below, in practical applications a PI speed loop provides an adequate estimate of τ_L . A scheme that removes this assumption has recently been proposed in Astolfi, Karagiannis and Ortega (2007).

3.5 Simulation results

The performance of the proposed SIDA–PBC was investigated by simulations considering two experiments described below. The considered motor parameters, taken from Ortega and Espinosa (1993), where $n_p = 1$, $L_s = 84$ mH, $L_r = 85.2$ mH, $L_{sr} = 81.3$ mH, $R_s = 0.687 \Omega$ and $R_r = 0.842 \Omega$, with a unitary rotor moment of inertia. Regarding the controller parameters, following field oriented ideas, the rotor flux equilibrium value was set to $x_{34\star} = \text{col}(\beta, 0)$ with $\beta = 2$, while $x_{12\star}$ were computed according to (16). In order to satisfy condition (28), $\mathcal{K}(\omega) = k(\omega)I_2$ was defined with

$$k(\omega) = \frac{L_{sr}}{(L_s L_r - L_{sr}^2)} [T_r^2 \omega^2 + 4].$$

In a first experiment the motor was initially at standstill with a zero load torque. At startup, the load torque was set to $\tau_L = 20$ Nm and this value was maintained until $t = 40$ sec when a new step in this variable was introduced changing to $\tau_L = 40$ Nm. Figure 1 shows the behaviour of the stator currents where it can be seen how, according to the field oriented approach, one of the stator currents remains (almost) constant while the second one is dedicated to producing the required generated torque. In this sense, Figure 2 shows how the

rotor flux is aligned with the reference frame since one of the components equals β while the other is zero. The internal stability of the closed-loop system is illustrated in Figure 3 where the rotor speed is presented. As expected, besides its boundedness, it can be seen that,

when the load torque is increased, this variable decreases. In Figure 4 the main objective of the proposed controller is depicted. Here it is shown how the generated torque regulation objective, both before and after the load torque change, is achieved.

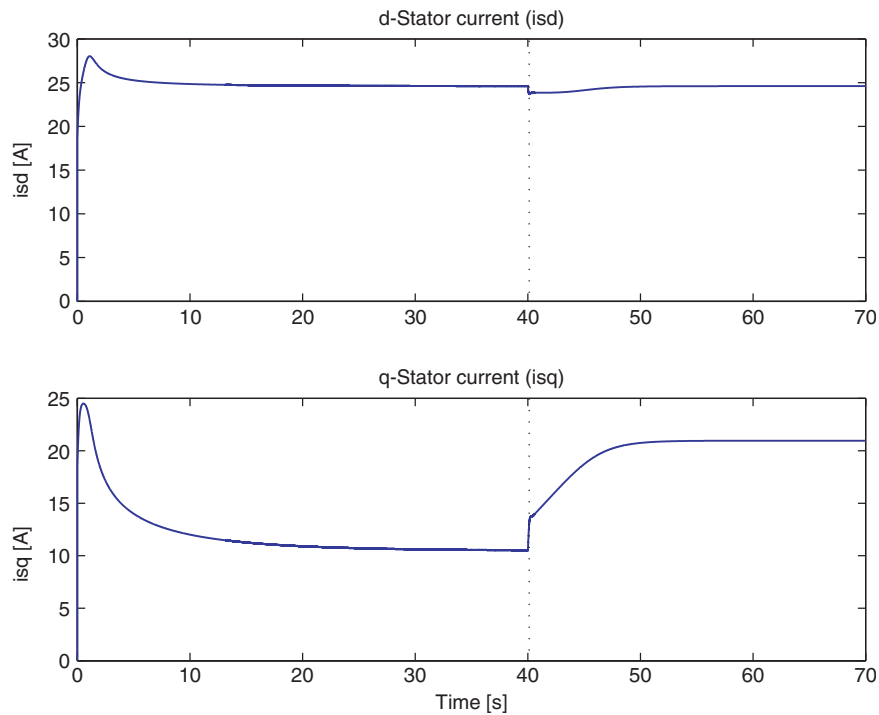


Figure 1. Stator currents.

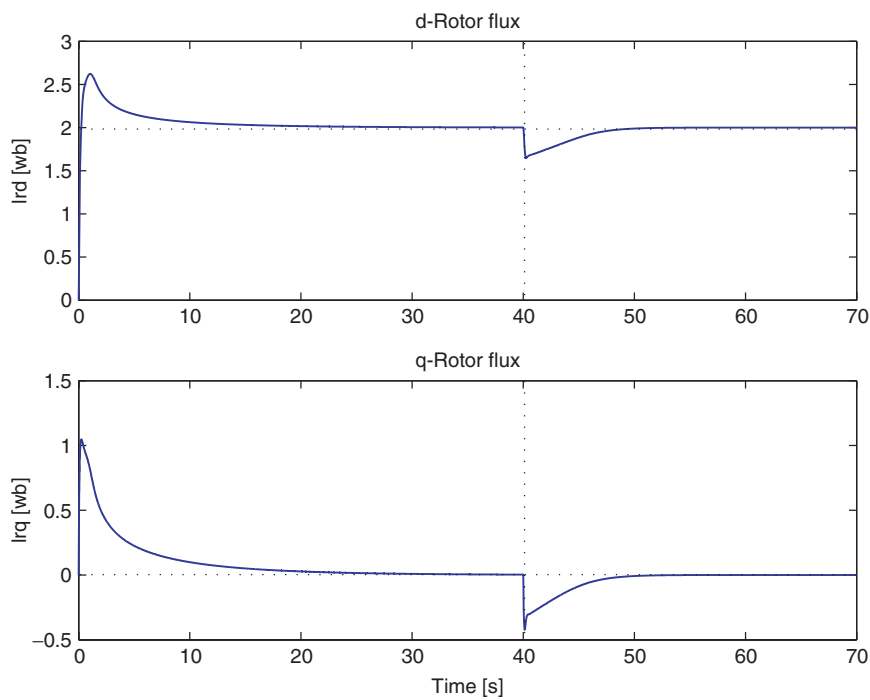


Figure 2. Rotor fluxes.

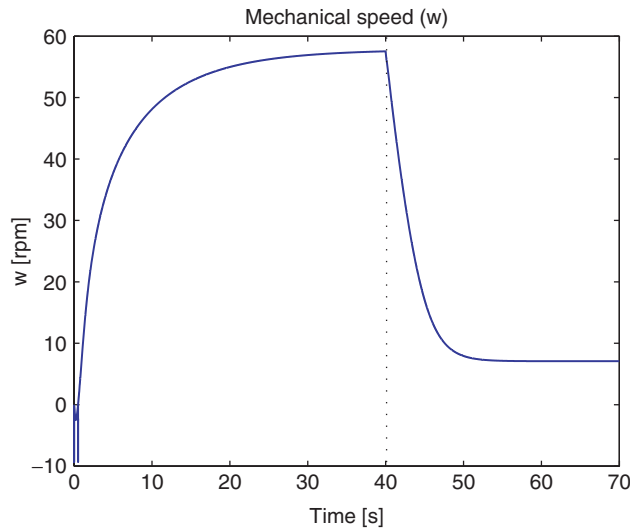


Figure 3. Rotor speed.

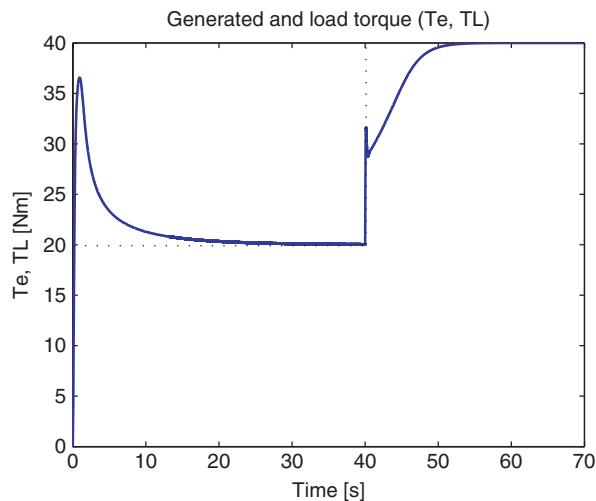


Figure 4. Generated (continuous line) and load (dashed line) torque.

Figure 5 shows the boundedness of the control (stator voltages) inputs.

The second experiment was aimed to illustrate the claim stated in Remark 4. In this sense, the control input u_3 was set to

$$u_3 = \hat{u}_{3\star} = R_r \frac{\hat{y}_{1\star}}{y_{2\star}},$$

where the estimate of the load torque is obtained as the output of a PI controller, defined over the speed error between the actual and the desired velocities, of the form

$$\hat{y}_{1\star}(t) = k_p(\omega(t) - \omega_\star) + k_i \int_0^t (\omega(s) - \omega_\star) ds$$

Figure 6 shows the rotor speed behaviour when the desired velocity is (initially) $\omega_\star = 100$ rpm and at

$t = 50$ sec it is changed to $\omega_\star = 150$ rpm. In this simulation it was considered $\tau_L = 10$ Nm, $k_i = -0.1$ and $k_p = -1$. All the other parameters were the same as in the first experiment.

4. Total energy-shaping of a doubly-fed induction generator

Doubly-fed induction machines (DFIM) have been proposed in the literature, among other applications, for high performance energy storage systems, wind-turbine generators or hybrid engines – (see Peresada, Tilli and Tonelli (2004) for an extended discussion). In Batlle et al. (2005) we considered a DFIM – controlled through the rotor voltage and connected to a variable local load – that acts as an energy-switching device between a local energy storing element (a flywheel) and the electrical power network. The control objective is to change the direction of the power flow (towards or from the flywheel) depending on the load demand. This is achieved by commuting between two different controllers that drive the system towards two given steady-state regimes. The equilibria associated to these regimes is stabilised with IDA–PBCs that, similar to the induction motor controller proposed in the previous section, shape the electrical energy, treating the mechanical dynamics as a cascaded subsystem.

The nested-loop architecture, with an inner-loop to control the electrical subsystem and an outer-loop (usually a simple PI) to control the mechanical variables, is prevalent in classical electromechanical systems applications, where it is justified to invoke time-scale separation arguments. Intrinsic to the nested-loop configuration is the fact that the time response of the mechanical subsystem is subordinated to the electrical transient. This may lead to below-par performances in small stand-alone DFIM-based generating units where a fast response of the mechanical speed is needed to ensure efficient control of the power flow and, furthermore, the mechanical and electrical time constants may be close. The purpose of this section is to show that, using SIDA–PBC, it is possible to shape the energy function of the complete system dynamics, resulting in a controller with improved power-flow regulation performance. To the best of our knowledge, this is the first control algorithm for this class of systems that provides for this additional degree of freedom.

4.1 Overall system model and equilibria

We consider the configuration for the DFIM studied in Batlle et al. (2005) to which we refer the reader for additional details. Here, we will concentrate on the problem of stabilisation of equilibria of the overall system.

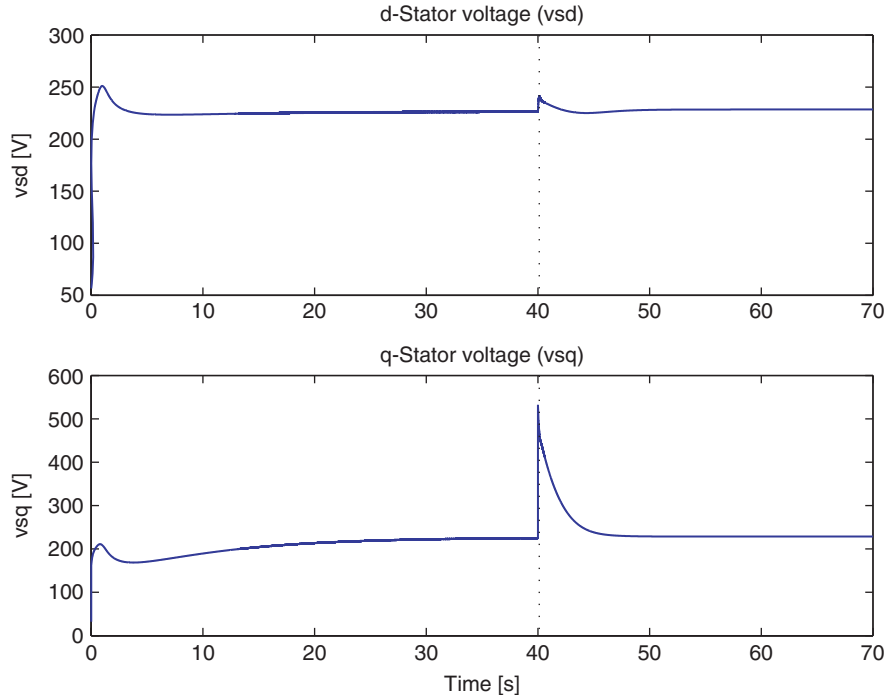


Figure 5. Stator voltages.

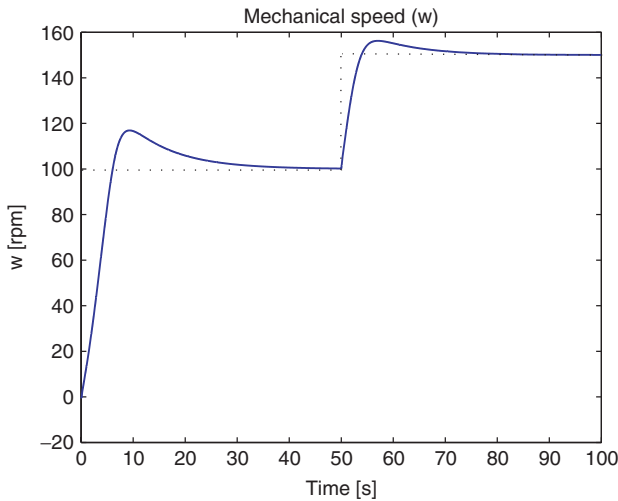


Figure 6. Speed behaviour.

Before presenting the systems model a word on notation is in order. We chose a representation in the dq framework rotating at the (constant) angular speed of the AC source (ω_s), and state vector $z = \text{col}(\lambda_s, \lambda_r, J_m \omega) \in \mathbb{R}^5$, where $\lambda_s, \lambda_r \in \mathbb{R}^2$ are the stator and rotor fluxes, respectively, $\omega \in \mathbb{R}$ is the mechanical speed, and J_m is the machine inertia. To simplify the derivations it will be convenient to work with a mixed notation, also writing some of the equations using the coordinates $\chi = \text{col}(i_s, i_r, \omega) \in \mathbb{R}^{5 \times 5}$, where $i_s, i_r \in \mathbb{R}^2$ are the stator

and rotor currents, respectively. The relation between z and χ is given by

$$z = \mathcal{L}\chi, \tag{30}$$

with

$$\mathcal{L} = \begin{bmatrix} L_s I_2 & L_{sr} I_2 & O_{2 \times 1} \\ L_{sr} I_2 & L_r I_2 & O_{2 \times 1} \\ O_{1 \times 2} & O_{1 \times 2} & J_m \end{bmatrix} = \mathcal{L}^\top > 0,$$

the generalised inductance matrix, where L_s, L_r, L_{sr} are the DFIM inductances.

The energy function of the overall system is $H(z) = (1/2)z^\top \mathcal{L}^{-1}z$, and the model given by

$$\dot{z} = [J(i_s, \omega) - R]\nabla H + \begin{bmatrix} v_s \\ O_{2 \times 1} \\ \tau_L \end{bmatrix} + \begin{bmatrix} O_{2 \times 2} \\ I_2 \\ O_{1 \times 2} \end{bmatrix} u, \tag{31}$$

where $v_s \in \mathbb{R}^2, \tau_L \in \mathbb{R}$ are, respectively, the stator voltage and the external mechanical torque, which are constant, and $u \in \mathbb{R}^2$ are the rotor voltages that act as control inputs.³ The structure and damping matrices are

$$J(i_s, \omega) := \begin{bmatrix} -\omega_s L_s \mathcal{J} & -\omega_s L_{sr} \mathcal{J} & O_{2 \times 1} \\ -\omega_s L_{sr} \mathcal{J} & -(\omega_s - \omega) L_r \mathcal{J} & L_{sr} \mathcal{J} i_s \\ O_{1 \times 2} & L_{sr} i_s^\top \mathcal{J} & 0 \end{bmatrix} = -J^\top(i_s, \omega),$$

$$R := \begin{bmatrix} R_s I_2 & O_{2 \times 2} & O_{2 \times 1} \\ O_{2 \times 2} & R_r I_2 & O_{2 \times 1} \\ O_{1 \times 2} & O_{1 \times 2} & B_r \end{bmatrix} > 0,$$

where R_s , R_r are DFIM resistances and B_r is the friction coefficient. All parameters, including B_r , are strictly positive.

Clearly, the fixed point equations for (31) are given by $z_\star = \mathcal{L}\chi_\star$, with $\chi_\star := \text{col}(i_{s\star}, i_{r\star}, \omega_\star)$ the solutions of

$$\left. \begin{aligned} -(\omega_s L_s \mathcal{J} + R_s I_2) i_{s\star} - \omega_s L_{sr} \mathcal{J} i_{r\star} + v_s &= 0 \\ L_{sr} i_{s\star}^\top \mathcal{J} i_{r\star} - B_r \omega_\star + \tau_L &= 0, \end{aligned} \right\} \quad (32)$$

which constitute a set of three non-linear algebraic equations in the variables $i_{s\star}$, ω_\star . As thoroughly discussed in Batlle et al. (2005), the direction of the power flow – towards or from the inertia wheel – can be regulated commuting between two controllers that stabilise two different equilibrium points. We will assume in the sequel that the desired equilibrium z_\star (or, correspondingly, χ_\star) is given and concentrate on the task of designing a SIDA–PBC that stabilises this equilibrium point.

4.2 SIDA–PBC design

As in Section 3 we will design our SIDA–PBC adopting the algebraic approach. For, we fix the desired energy function as

$$H_d(z) = \frac{1}{2}(z - z_\star)^\top P(z - z_\star), \quad P = P^\top > 0. \quad (33)$$

The SIDA–PBC design reduces to finding a matrix $F_d(z)$ solution of

$$[J(i_s, \omega) - R] \nabla H + \begin{bmatrix} v_s \\ O_{3 \times 1} \end{bmatrix} + \begin{bmatrix} O_{2 \times 2} \\ I_2 \\ O_{1 \times 2} \end{bmatrix} u = F_d(z) P(z - z_\star), \quad (34)$$

and verifying $F_d(z) + F_d^\top(z) \leq 0$. To simplify the solution we restrict P to being diagonal and (for reasons that will become clear below impose) the {13}-element of $F_d(z)$ to be zero, that is,

$$P = \begin{bmatrix} p_s I_2 & O_{2 \times 2} & O_{2 \times 1} \\ O_{2 \times 2} & p_r I_2 & O_{2 \times 1} \\ O_{1 \times 2} & O_{1 \times 2} & p_\omega \end{bmatrix} > 0, \\ F_d(z) = \begin{bmatrix} F_{11}(z) & F_{12}(z) & O_{2 \times 1} \\ F_{21}(z) & F_{22}(z) & F_{23}(z) \\ F_{31}^\top(z) & F_{32}^\top(z) & F_{33}(z) \end{bmatrix},$$

where the partition of $F_d(z)$ is conformal with the partition of P .

From the first two rows of (34), after using (30) and the first equation in (32), one obtains

$$\begin{aligned} -(\omega_s L_s \mathcal{J} + R_s I_2) \tilde{i}_s - \omega_s L_{sr} \mathcal{J} \tilde{i}_r &= (L_s F_{11} p_s + L_{sr} F_{12} p_r) \tilde{i}_s \\ &+ (L_{sr} F_{11} p_s + L_r F_{12} p_r) \tilde{i}_r, \end{aligned}$$

which, for all \tilde{i}_s, \tilde{i}_r , has a unique solution given by

$$F_{11} = -\frac{1}{p_s} \left(\omega_s \mathcal{J} + \frac{L_r}{\mu} R_s I_2 \right) \quad (35)$$

$$F_{12} = \frac{L_{sr}}{p_r \mu} R_s I_2, \quad (36)$$

where $\mu := L_s L_r - L_{sr}^2 > 0$.

We remark that this simple calculation was possible because the element F_{13} of $F_d(z)$ was set to zero. The price paid for having this term equal to zero is that it makes the selection of $F_{31}(z)$ critical. Indeed, this term will appear in the corners of $F_d(z) + F_d^\top(z)$, that we recall should be negative semi-definite. The term $F_{32}(z)$, on the other hand, is not critical because its contribution to $F_d(z) + F_d^\top(z)$ can be countered by a suitable selection of $F_{23}(z)$ that, in view of the presence of the control, is totally free. These issues will become clearer as we go through the calculations below.

From the fifth row of (34) and (30) we get

$$\begin{aligned} [F_{31}^\top(z) p_s \quad F_{32}^\top(z) p_r \quad F_{33}(z) p_\omega] \mathcal{L} \tilde{x} \\ = L_{sr} i_s^\top \mathcal{J} i_r - B_r \omega \\ = L_{sr} [-i_{r\star}^\top \mathcal{J} \quad i_s^\top \mathcal{J}] \tilde{i} - B_r \tilde{\omega} \end{aligned}$$

with the second identity obtained adding and subtracting the equilibrium Equation (32). From the $\tilde{\omega}$ term we get

$$F_{33} = -\frac{B_r}{p_\omega J_m}, \quad (37)$$

while the remaining equations can be arranged as

$$\tilde{i}^\top \left(L \begin{bmatrix} p_s F_{31}(z) \\ p_r F_{32}(z) \end{bmatrix} - L_{sr} \begin{bmatrix} \mathcal{J} i_{r\star} \\ -\mathcal{J} i_s \end{bmatrix} \right) = 0, \quad (38)$$

where we have defined

$$L := \begin{bmatrix} L_s I_2 & L_{sr} I_2 \\ L_{sr} I_2 & L_r I_2 \end{bmatrix}.$$

Although a solution for $F_{31}(z)$ and $F_{32}(z)$ of this equation can be easily obtained – inverting L to set the term inside the parenthesis equal to zero – it turns out that we don't have enough flexibility in the control to generate a matrix $F_d(z)$ that satisfies the skew-symmetry constraint (4), and we have to look for an alternative solution. Towards this end, notice that we can add to (38) any vector $G(z) \in \mathbb{R}^4$

$$\tilde{i}^\top \left(L \begin{bmatrix} p_s F_{31}(z) \\ p_r F_{32}(z) \end{bmatrix} - L_{sr} \begin{bmatrix} \mathcal{J} i_{r\star} \\ -\mathcal{J} i_s \end{bmatrix} - G(z) \right) = 0 \quad (39)$$

as long as

$$\tilde{i}^\top G(z) = 0.$$

Setting the term inside the parenthesis of (39) equal to zero we get

$$\begin{bmatrix} p_s F_{31}(z) \\ p_r F_{32}(z) \end{bmatrix} = \frac{L_{sr}}{\mu} \begin{bmatrix} L_r \mathcal{J} i_{r*} + L_{sr} \mathcal{J} i_s \\ -L_r \mathcal{J} i_s - L_{sr} \mathcal{J} i_{r*} \end{bmatrix} + \begin{bmatrix} G_C(z) \\ G_D(z) \end{bmatrix}, \quad (40)$$

where, for convenience, we have introduced the partition

$$\begin{bmatrix} G_C(z) \\ G_D(z) \end{bmatrix} = L^{-1} G(z)$$

with $G_C(z), G_D(z) \in \mathbb{R}^2$. As indicated above, to satisfy the skew-symmetry condition it is necessary to generate a solution with $F_{31}(z)$ constant. This is easily achieved selecting

$$G_C(z) = -\frac{L_{sr}^2}{\mu} \mathcal{J} \tilde{i}_s. \quad (41)$$

With this selection $G(z)$ results in

$$G(z) = \begin{bmatrix} -\frac{L_{sr}^2 L_r}{\mu} \mathcal{J} \tilde{i}_s + L_{sr} G_D \\ -\frac{L_{sr}^3}{\mu} \mathcal{J} \tilde{i}_s + L_r G_D \end{bmatrix}$$

and, in order to ensure $\tilde{i}^\top G(z) = 0$, we fix

$$G_D(z) = -\frac{L_{sr}^2}{\mu} \mathcal{J} \tilde{i}_r. \quad (42)$$

Finally, replacing (41) and (42) in (40) we get

$$\left. \begin{aligned} F_{31} &= \frac{L_{sr}}{p_s \mu} \mathcal{J} (L_{sr} i_{s*} + L_r i_{r*}) = \frac{L_{sr}}{p_s \mu} \mathcal{J} \lambda_{r*} \\ F_{32}(z) &= -\frac{L_{sr}}{p_r \mu} \mathcal{J} (L_s i_s + L_{sr} i_r) = -\frac{L_{sr}}{p_r \mu} \mathcal{J} \lambda_s \end{aligned} \right\} \quad (43)$$

The next step is to select the remaining terms of $F_d(z)$, that are directly affected by the control action, to satisfy the skew-symmetry constraint (4). To simplify the condition, we select

$$F_{21} = -F_{12}, \quad F_{23}(z) = -F_{32}(z), \quad F_{22} = -\frac{k_r}{2p_r} I_2 < 0$$

which yields

$$F_d(z) + F_d^\top(z) = \begin{bmatrix} -\frac{2L_r R_s}{p_s \mu} I_2 & O_{2 \times 2} & \frac{L_{sr}}{p_s \mu} \mathcal{J} \lambda_{r*} \\ O_{2 \times 2} & -\frac{k_r}{p_r} I_2 & O_{2 \times 1} \\ -\frac{L_{sr}}{p_s \mu} \lambda_{r*}^\top \mathcal{J} & O_{1 \times 2} & -\frac{2B_r}{p_\omega J_m} \end{bmatrix}. \quad (44)$$

A simple Schur's complement analysis establishes that $F_d(z) + F_d^\top(z) < 0$ if and only if the free parameters p_s and p_ω satisfy

$$p_s > \left(\frac{J_m L_{sr}^2}{4B_r L_r R_s \mu} |\lambda_{r*}|^2 \right) p_\omega. \quad (45)$$

Remark 6: The inequality (45) clearly reveals the critical role played by B_r . If this parameter is small (p_s/p_ω) has to be large. In the next section we compute the control law and we see that this can be achieved injecting a high gain in the current loop or reducing the gain on the speed error feedback, both options inducing obvious detrimental effects.

4.3 Proposed controller and stability analysis

Once we have solved the SIDA-PBC matching equations, the design is completed, computing the controller and assessing its stability properties. This is summarised in the proposition below.

Proposition 3: Consider the DFIM system (31) in closed-loop with the static feedback control

$$\begin{aligned} u &= R_r i_r + (\omega_s - \omega) \mathcal{J} (L_{sr} i_s + L_r i_r) - k_s (L_s \tilde{i}_s + L_{sr} \tilde{i}_r) \\ &\quad - k_r (L_{sr} \tilde{i}_s + L_r \tilde{i}_r) + k_\omega \mathcal{J} \lambda_s \tilde{\omega}, \end{aligned} \quad (46)$$

where $k_r > 0, k_\omega > 0$ and

$$k_s > \frac{L_{sr}^2}{4B_r L_r \mu} |\lambda_{r*}|^2 k_\omega.$$

The closed-loop system is then described by $\dot{z} = F_d(z) \nabla H_d$, with $H_d(z)$ defined in (33), and $F_d(z) + F_d^\top(z) < 0$. Consequently, the equilibrium z_* is globally exponentially stable.

Proof: From the second row of (34) we obtain

$$\begin{aligned} u &= R_r i_r + (\omega_s - \omega) \mathcal{J} (L_{sr} i_s + L_r i_r) + F_{21} p_s \tilde{\lambda}_s + F_{22} p_r \tilde{\lambda}_r \\ &\quad + F_{23}(z) p_\omega J_m \tilde{\omega}. \end{aligned}$$

The control law (46) follows from this expression after substitution of the values of F_{ij} , using (30) and defining

$$k_s := \frac{p_s L_{sr} R_s}{p_r \mu}, \quad k_\omega := \frac{p_\omega J_m L_{sr}}{p_r \mu}.$$

Finally, the lower bound on (k_s/k_ω) is obtained from the inequality (45). \square

4.4 Adaptive control scheme

In this subsection we present an adaptive control scheme in order to robustify the controller obtained via the SIDA-PBC technique. As seen in (46), the control

law has an strong dependence on R_r , which, in general, is an uncertain parameter.

We propose here a classical adaptation scheme. Replacing (46) by

$$u = (\omega_s - \omega)\mathcal{J}(L_{sr}\tilde{i}_s + L_r i_r) - k_s(L_s\tilde{i}_s + L_{sr}\tilde{i}_r) - k_r(L_{sr}\tilde{i}_s + L_r\tilde{i}_r) + k_\omega\mathcal{J}\lambda_s\tilde{\omega} + \hat{R}_r i_r, \quad (47)$$

where \hat{R}_r is an estimate of R_r that we have to generate on-line, we define the parameter error $\tilde{R}_r = \hat{R}_r - R_r$. The closed-loop system has the form

$$\dot{z} = F\nabla H_d + \tilde{R}_r B i_r,$$

where

$$B = \begin{bmatrix} O_{2 \times 2} \\ I_2 \\ O_{1 \times 2} \end{bmatrix}.$$

To complete the design we propose a Lyapunov function

$$W(z, \tilde{R}_r) = H_d + \frac{1}{2k_a} \tilde{R}_r^2,$$

where $k_a > 0$ is the adaptation gain. Its derivative yields

$$\dot{W} = -(\nabla H_d)^\top F \nabla H_d + (\nabla H_d)^\top B i_r \tilde{R}_r + \frac{1}{k_a} \tilde{R}_r \dot{\tilde{R}}_r.$$

Selecting $\dot{\tilde{R}}_r = -k_a (\nabla H_d)^\top B i_r$ one gets

$$\dot{W} = -(\nabla H_d)^\top F \nabla H_d \leq 0,$$

so that stability is proved. The obtained adaptation law is

$$\dot{\tilde{R}}_r = -k_a (L_{sr}\tilde{i}_s^\top - L_r\tilde{i}_r^\top) p_r i_r.$$

4.5 Simulations

In this subsection we present some simulations using the DFIM parameters of Batlle et al. (2005). That is (in SI units) $L_s = L_r = 0.011$, $L_{sr} = 0.01$, $R_r = R_s = 0.01$, $J_m = 0.001$, $B_r = 0.005$, $v_s = \text{col}(380, 0)$ and $\omega_s = 2\pi \times 50$. The controller parameters are selected as $k_s = 1000$, $k_r = 100$ and $k_\omega = 0.01$.

The first numerical experiment is performed using the DFIM as a motor (for $0 < t \leq 0.5$). In this case $\tau_L = -5$ and the desired speed is $\omega_\star = 320$ for $0 < t \leq 0.25$ and $\omega_\star = 305$ for $0.25 < t \leq 0.5$. The second simulation is done using the DFIM as a generator (for $0.5 < t \leq 1$). In this case $\tau_L = 5$ and the desired current is $i_{s\star} = \text{col}(-2.7, 0)$ for $0.5 < t \leq 0.75$ and $i_{s\star} = \text{col}(-2.85, 0)$ for $0.75 < t \leq 1$. Notice that, to improve the power factor, we have set the second (q) component of $i_{s\star}$ to zero. The behaviour of the mechanical speed and the d and q -components of the stator current for both simulations are depicted in Figures 7, 8 and 9, respectively.

In Figure 10 we compare the speed behaviour of the new SIDA-PBC with the IDA-PBC reported in Batlle et al. (2005) – that shapes only the

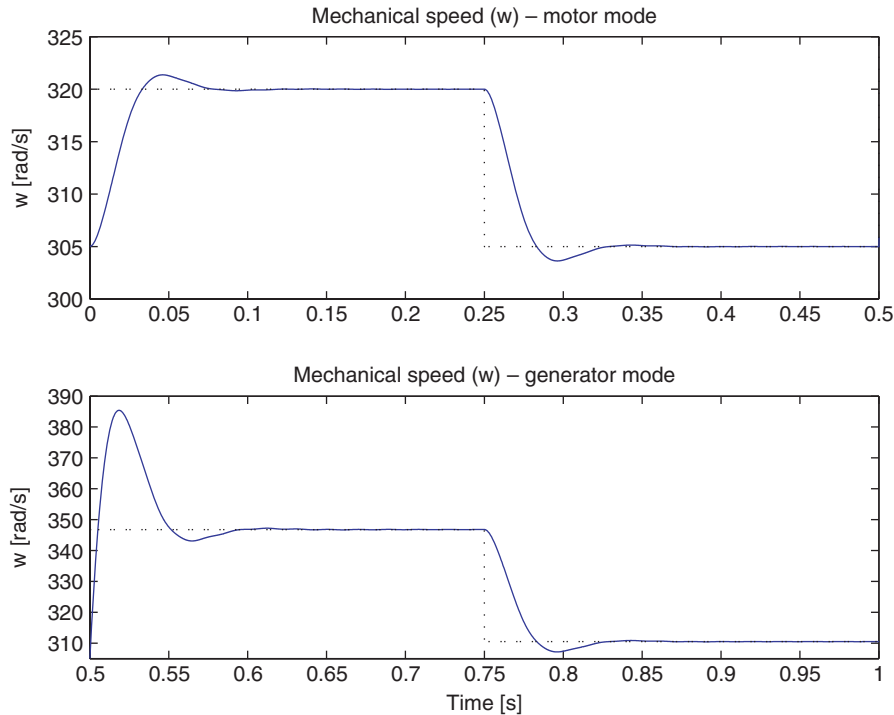


Figure 7. Mechanical speed, ω .

electrical energy. The simulation conditions are the same as before but, in view of the slower response of the controller of Batlle et al. (2005), we had to scale up the time. As expected, in spite of the large damping

coefficient used in the IDA-PBC ($r=1000$), SIDA-PBC achieves a much faster speed response.

To evaluate the adaptive controller (47) the same experiment as before is repeated but now varying the

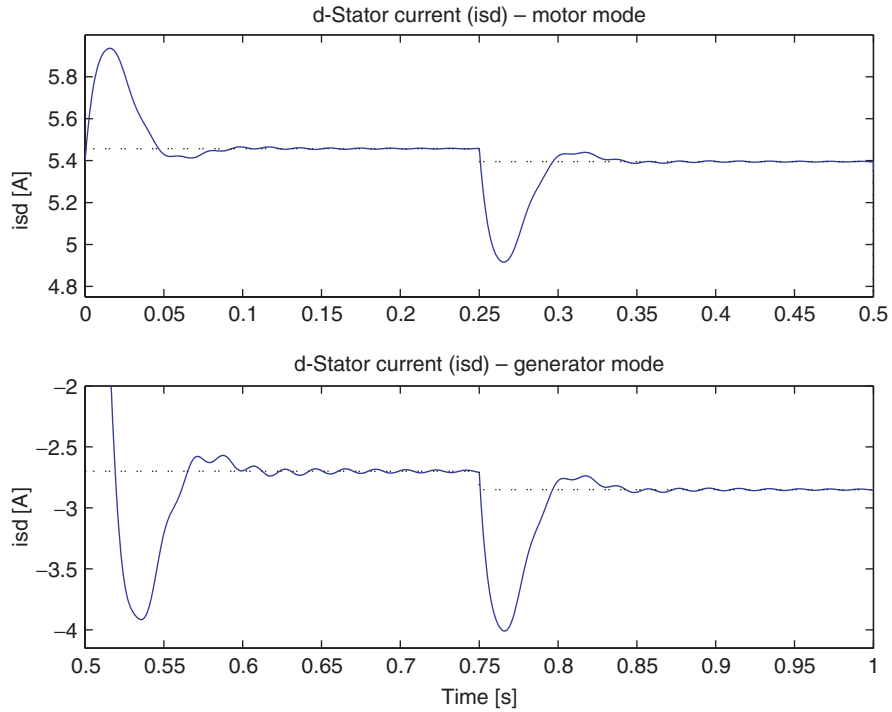


Figure 8. Stator current d -component.

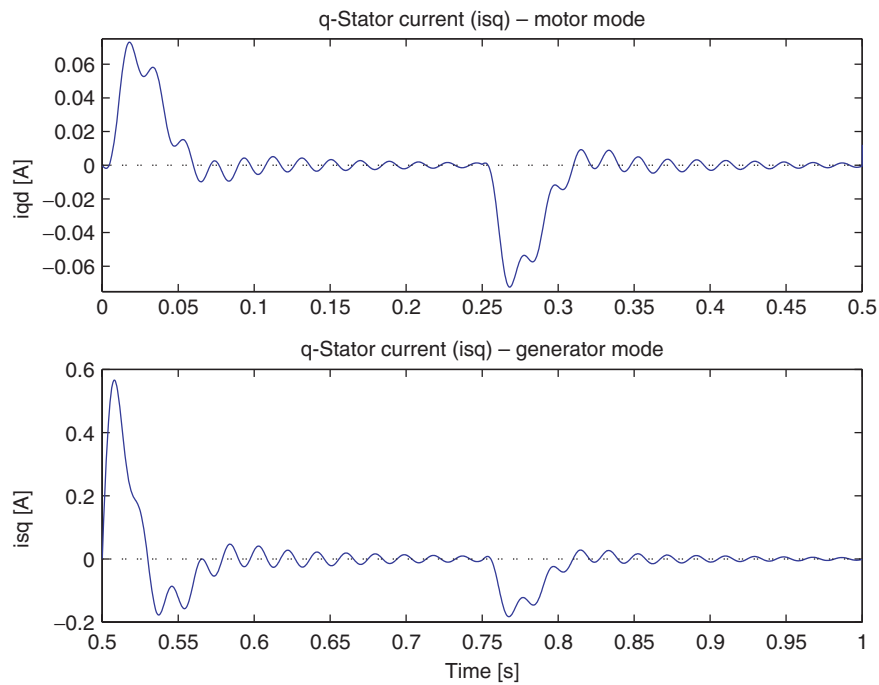


Figure 9. Stator current q -component.

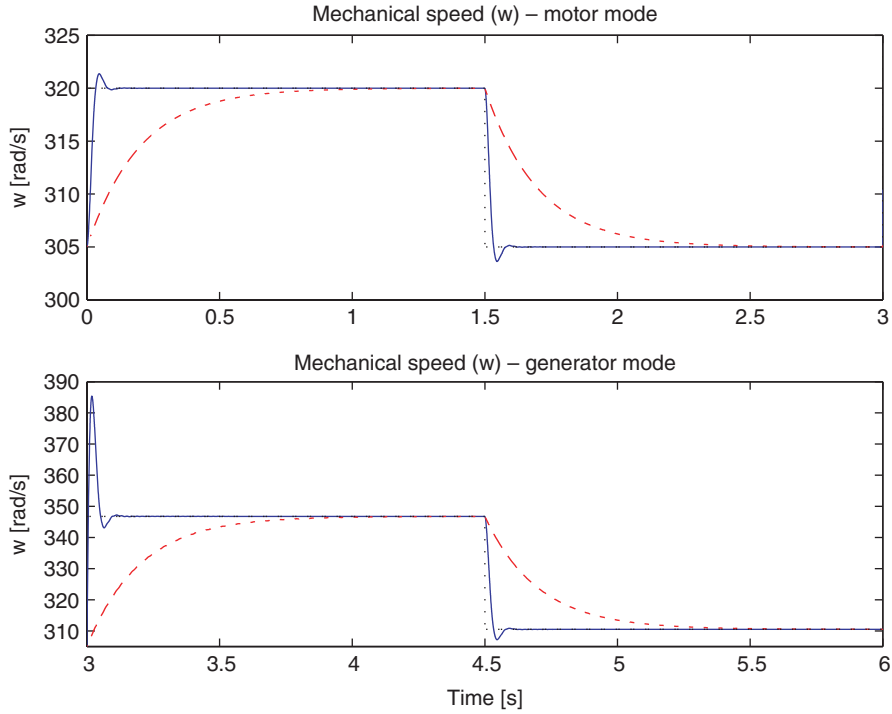


Figure 10. Mechanical speed, ω , for SIDA-PBC (continuous line) and IDA-PBC (dashed line).

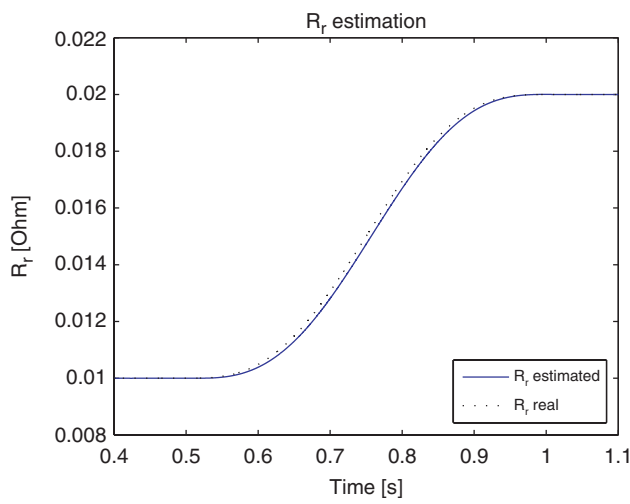


Figure 11. Rotor resistance estimation, \hat{R}_r .

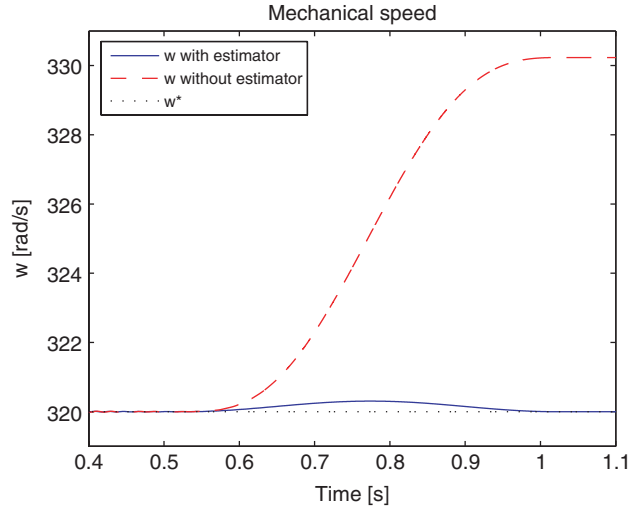


Figure 12. Mechanical speed, with and without estimator.

rotor resistance parameter R_r . At $t=0.5$ s the value of R_r of the model is smoothly increased to $R_r=0.02$, simulating temperature effects. Figures 11 and 12 show the estimation behaviour of \hat{R}_r and the dynamics of the mechanical speed, respectively. The convergence of the estimated value of \hat{R}_r to the real value (Figure 11) ensures that the performance of the ideal system is recovered (Figure 12).

5. Conclusions and future work

We have presented an extension of the highly successful IDA-PBC methodology, called SIDA-PBC, where the energy-shaping and damping injection tasks are not performed sequentially, but simultaneously. In this way we enlarge the class of systems that can be stabilised using PBC and, furthermore, through the consideration of a broader set of desired damping

matrices, we provide the designer with more tuning knobs to improve performance.

This new idea has been applied to solve the long standing problem of IDA–PBC of induction motors, that turns out to be unsolvable with a two stage design. Also, by avoiding the classical nested-loop control configuration prevalent in electromechanical systems, we have been able to improve the mechanical response of a DFIM, working both as a motor and a generator.

Concerning future research, it is the authors' belief that additional advantages can be obtained from the solution of the matching equation, specially from an implementation perspective, for example by designing output feedback control schemes. Regarding the induction machine, experimental validation of the two proposed control algorithms is currently being terminated and will be reported in the near future.

Acknowledgements

This work has been done in the context of the European sponsored project Geoplex with reference code IST-2001-34166. Further information is available at <http://www.geoplex.cc>. The work of Carles Batlle, Arnau Dòria-Cerezo and Gerardo Espinosa has been (partially) supported by the Spanish projects MTM 2007-62480, DPI 2007-62582 and CONACyT (51050) and DGAPA-UNAM (IN112908), respectively.

Notes

1. All vectors in the paper are column vectors, even the gradient of a scalar function denoted $\nabla_{(\cdot)} = (\partial/\partial(\cdot))$. When clear from the context the subindex will be omitted.
2. That is, x_* is a member of the set $\{\bar{x} \in \mathbb{R}^n \mid g^\perp(\bar{x})f(\bar{x}, t) = 0, \forall t \in \mathbb{R}\}$.
3. We underscore the difference of the DFIM with respect to the classical (squirrel cage) induction motor (see, e.g., previous section) where the control signals are the stator voltages and the rotor is short-circuited. Also, in DFIM both rotor and stator currents are available for measurement.

References

- Astolfi, A., Karagiannis, D., and Ortega, R. (2007), *Nonlinear and Adaptive Control with Applications*, Berlin: Springer-Verlag, Communications and Control Engineering.
- Batlle, C., Dòria-Cerezo, A., and Ortega, R. (2005), 'Power Flow Control of a Doubly-fed Induction Machine Coupled to a Flywheel', *European Journal of Control*, 11, 209–221.
- Dawson, D., Hu, J., and Burg, T. (1998), *Nonlinear Control of Electric Machinery*, New York: Marcel Dekker.
- Fujimoto, K., and Sugie, T. (2001), 'Canonical Transformations and Stabilisation of Generalised Hamiltonian Systems', *Systems and Control Letters*, 42, 217–227.
- Krause, P.C., Wasynczuk, O., and Sudhoff, S.D. (1995), *Analysis of Electric Machinery*, USA: IEEE Press.
- Marino, R., Peresada, S., and Valigi, P. (1993), 'Adaptive Input–output Linearizing Control of Induction Motors', *IEEE Transactions on Automatic Control*, 38, 208–221.
- Ortega, R., and Garcia-Canseco, E. (2004), 'Interconnection and Damping Assignment Passivity-Based Control: A Survey', *European Journal of Control*, 10, 432–450.
- Ortega, R., and Espinosa, G. (1993), 'Torque Regulation of Induction Motors', *AUTOMATICA*, 29, 621–633.
- Ortega, R., Spong, M., Gomez, F., and Blankenstein, G. (2002a), 'Stabilisation of Underactuated Mechanical Systems via Interconnection and Damping Assignment', *IEEE Transactions on Automatic Control*, 47, 1218–1233.
- Ortega, R., van der Schaft, A., Maschke, B., and Escobar, G. (2002b), 'Interconnection and Damping Assignment Passivity-based Control of Port-controlled Hamiltonian Systems', *AUTOMATICA*, 38, 585–596.
- Ortega, R., Loria, A., Nicklasson, P.J., and Sira-Ramírez, H. (1998), *Passivity-based Control of Euler–Lagrange Systems*, Berlin: Springer-Verlag, Communications and Control Engineering.
- Peresada, S., Tilli, A., and Tonelli, A. (2004), 'Power Control of a Doubly-fed Induction Machine via Output Feedback', *Control Engineering Practice*, 12, 41–57.
- Prajna, S., van der Schaft, A., and Meinsma, G. (2002), 'An LMI Approach to Stabilisation of Linear Port-controlled Hamiltonian Systems', *Systems & Control Letters*, 42, 371–385.
- Rodriguez, H., and Ortega, R. (2003), 'Interconnection and Damping Assignment Control of Electromechanical Systems', *International Journal of Robust and Nonlinear Control*, 13, 1095–1111.
- Sepulchre, R., Janković, M., and Kokotović, P. (1997), *Constructive Nonlinear Control*, London: Springer-Verlag.
- Takegaki, M., and Arimoto, S. (1981), 'A New Feedback for Dynamic Control of Manipulators', *Transactions of the ASME: Journal of Dynamic Systems, Measurement and Control*, 102, 119–125.
- van der Schaft, A. (2002), *L₂-Gain and Passivity Techniques in Nonlinear Control* (2nd ed.), London: Springer Verlag.